PPP2R2D, a regulatory subunit of protein phosphatase 2A, promotes gastric cancer growth and metastasis via mechanistic target of rapamycin activation

SHIJUN YU[1], LI LI[1], QIONG WU[1], NING DOU[1], YANDONG LI[1,2] and YONG GAO[1]

[1]Department of Oncology, Shanghai East Hospital, Tongji University School of Medicine, Shanghai 200120;
[2]Research Center for Translational Medicine, Shanghai East Hospital,
Tongji University School of Medicine, Shanghai 200120, P.R. China

Received November 12, 2017; Accepted March 15, 2018

DOI: 10.3892/ijo.2018.4329

Abstract. Protein phosphatase 2A (PP2A) is an essential serine/threonine protein phosphatase that regulates the basic activities of eukaryotes by dephosphorylating its substrates. The function and substrate specificity of PP2A are generally determined by its regulatory subunits. In the present study, the clinical significance and roles of PPP2R2D, one of the regulatory subunits of PP2A, were demonstrated in gastric cancer (GC) carcinogenesis. Through a tissue microarray and quantitative polymerase chain reaction analysis, it was demonstrated that PPP2R2D was commonly upregulated in GC samples. This upregulation was positively correlated with the patients' tumor stage (P<0.01), T classification (P<0.01) and N classification (P=0.01). Furthermore, a high expression of PPP2R2D was closely associated with poor prognosis of patients. Knockdown of PPP2R2D significantly inhibited the proliferation and migration of GC cells *in vitro*, as well as the tumorigenicity and metastasis *in vivo* in an animal GC model. By contrast, overexpression of PPP2R2D promoted GC cell proliferation and migration *in vitro*. The analysis of underlying mechanisms indicated that PPP2R2D silencing decreased the phosphorylation level of mechanistic target of rapamycin (mTOR), thereby implicating that PPP2R2D is involved in the regulation of mTOR activity during tumorigenesis. Thus, the findings of the present study suggested that PPP2R2D may serve as a potential oncogene in GC and as a novel target for therapeutic strategies against this disease.

Correspondence to: Dr Yandong Li or Dr Yong Gao, Department of Oncology, Shanghai East Hospital, Tongji University School of Medicine, 150 Ji-Mo Road, Shanghai 200120, P.R. China
E-mail: yandongli2009@gmail.com
E-mail: drgaoyong@163.com

Key words: PPP2R2D, mechanistic target of rapamycin, gastric cancer, tumor growth, metastasis

Introduction

Controlled protein phosphorylation and dephosphorylation are fundamental in all aspects of biology (1), and the underlying mechanism is regulated by protein kinases and protein phosphatases (PPs). Protein phosphatase 2A (PP2A), a major serine/threonine phosphatase and critical member of the PP family, is ubiquitously expressed in eukaryotic cells. It serves a significant role in several essential cellular functions, including cell cycle regulation, cell growth, differentiation, metabolism and cell mobility (2-4). Dysregulation of PP2A is associated with numerous diseases, including human cancer.

PP2A is a large heterotrimeric holoenzyme consisting of a wide variety of regulatory subunits B, a structural subunit A, and a catalytic subunit C or PP2AC (5). The A subunits function as scaffold proteins that are responsible for the formation of the holoenzyme and for the stability of the complex. In addition, the regulatory B subunits include four subfamilies, namely B (PR55), B' (B56 or PR61), B'' (PR72) and B''' (PR93/PR110). Different families, isoforms and splice variants of the regulatory subunits determine the broad substrate specificity and allow the PP2A holoenzyme to selectively regulate signaling pathways (6). The B family of regulatory subunits are encoded by four genes known as PPP2R2s, including PPP2R2A (B55α), PPP2R2B (B55β), PPP2R2C (B55γ) and PPP2R2D (B55δ) (7), which exhibit temporal and spatial expression patterns. PPP2R2A and PPP2R2D are expressed ubiquitously in mammalian cells, while PPP2R2B and PPP2R2C are highly enriched in the brain (7-9).

PP2A has been reported to function as a potential tumor suppressor (10); however, this predominant perception has been challenged over the past decades. Certain studies indicated that the inactivation of PP2A induces apoptosis in a number of tissues and cell types, including the pancreas, testes, liver and leukemic cells (11-15). This accumulating evidence suggested a different role for PP2A in distinct cancer types. B subunits are key factors that determine the substrate specificity of PP2A and, among them, PPP2R2D is expressed ubiquitously in mammalian cells. Several investigators have thus revealed the association between PPP2R2D and human cancer. For instance, Zhuang *et al* (16) reported that PPP2R2D

enhanced the sensitivity of human hepatocellular carcinoma to chemotherapy. In addition, Cunningham *et al* (17) observed that knockdown of PPP2R2D increased cell death in pancreatic cancer cell lines. Although the aforementioned studies indicated that PPP2R2D may be involved in cancer progression, the precise function and clinical relevance of PPP2R2D in human cancer remain unknown.

Gastric cancer (GC) is one of the most common malignancies and the third leading cause of cancer-associated mortality worldwide (18). Its prognosis remains poor due to the advanced stage of cancer progression at the time of diagnosis. Thus, the identification of novel biomarkers for early stage diagnosis is an urgent requirement for GC. In the present study, the expression pattern and function of PPP2R2D in GC were investigated, and it was observed that it is frequently overexpressed in tumor tissues and its expression may indicate tumor progression and poor prognosis. Furthermore, evidence was provided that PPP2R2D is involved in GC cell proliferation and migration possibly through the mechanistic target of rapamycin (mTOR) signaling pathway.

Materials and methods

Human tissue sample collection. Human GC and adjacent gastric mucosa specimens were obtained from 28 patients following resection at the Shanghai East Hospital of Tongji University School of Medicine (Shanghai, China) between October 2013 and May 2014. Informed consent was obtained from all patients prior to the sample collection. Primary GC in the tissues of these patients was diagnosed according to the 7th criteria of The American Joint Committee on Cancer (19) and confirmed by at least two pathologists subsequent to the resection. All the samples were snap-frozen in liquid nitrogen and preserved at -80˚C prior to RNA extraction. Kaplan Meier Plotter database (http://kmplot.com) was used to assess the effects of PPP2R2D on the prognosis of GC. This study was approved by the Ethics Committee of Shanghai East Hospital, Tongji University School of Medicine.

Tissue microarray and immunohistochemistry staining. A human GC tissue microarray (HStmA180Su09) containing 90 patient tumor samples and adjacent gastric mucosa specimens were purchased from Outdo Biotech Co., Ltd. (Shanghai, China). The cohort comprised of 21 females and 69 males with an age range between 17 and 84 years. The overall survival (OS) duration of the patients was defined as the interval between initial surgery and mortality. The sample sections (4 μm) were prepared and processed for immunostaining using an antibody against PPP2R2D (ab181071; Abcam, Cambridge, MA, USA) at a dilution of 1:500. According to the percentage of positive cells, two pathologists blinded to the clinical information evaluated the intensity of PPP2R2D staining independently. The results were classified into the following categories: Negative (-), <15%; weakly positive (+), 15-40%; moderate positive (++), 40-75%; or strongly positive (+++), >75%.

Cell culture and reagents. Human GC cell lines MGC803, SGC7901, BGC823, MKN28, AGS and HGC27 were obtained from the Shanghai Cell Bank of the Chinese Academy of Sciences (Shanghai, China). Among these cell lines, MKN28 is a type of mixed gastric adenocarcinoma cell line derived from MKN74 cells (20); this does not affect the outcomes of the present study. Cells were cultured in Dulbecco's modified Eagle's medium (DMEM; Corning, Inc., Corning, NY, USA) supplemented with 10% fetal bovine serum (FBS) and 1% penicillin/streptomycin. All cell lines were maintained at 37˚C in a 5% CO_2 humidified incubator (Thermo Fisher Scientific, Inc., Waltham, MA, USA).

RNA extraction and quantitative polymerase chain reaction (qPCR). Total RNA was isolated from the cultured cells or tissues using RNAiso Plus reagent and 1 μg total RNA was reverse-transcribed into cDNA using the PrimeScript™ RT reagent kit (both from Takara Bio, Inc., Otsu, Japan) according to the manufacturer's protocol. The concentration of RNA was measured using a Thermo Fisher Scientific NanoDrop™ spectrophotometer (NanoDrop; Thermo Fisher Scientific, Inc., Wilmington, DE, USA). qPCR was performed with SYBR-Green reagent (Takara Bio, Inc.) on an ABI 7500 Real-Time PCR system (Thermo Fisher Scientific, Inc.). The qPCR thermocycling conditions were: Initial hold at 95˚C for 10 min, followed by 40 cycles of denaturation at 95˚C for 15 sec and annealing/extension at 60˚C for 60 sec. The primer sequences used were as follows: PPP2R2D, 5'-CGAGTA CCTGCGCAGCAAGCT-3' (forward) and 5'-GACCCGGTC ATGATGGCGCTATC-3' (reverse); β-actin, 5'-CCTGGCACC CAGCACAATG-3' (forward) and 5'-GGGCCGGACTCG TCATACT-3' (reverse). β-actin served as an internal control, and the $2^{-\Delta\Delta Ct}$ method (21) was used for mRNA level quantification.

Western blot analysis. GC cells were lysed in lysis buffer (containing 25 mM Tris-Cl, pH 7.5, 1% SDS and 5 mM EDTA) supplemented with protease inhibitor cocktail (Sigma-Aldrich; Merck KGaA, Darmstadt, Germany) for 30 min on ice. For phosphorylated protein, 1% phosphatase inhibitor cocktail (Sigma-Aldrich; Merck KGaA) was added to the lysis buffer. Total protein was assessed using Bicinchoninic Acid Protein Assay kit (Beyotime Institute of Biotechnology, Haimen, China). Prior to the standard western blot analysis, protein lysates were diluted in 5X SDS loading buffer and boiled for 3 min. Total protein extracts (30-50 μg) were electrophoresed by 10% SDS-PAGE and transferred onto a polyvinylidene difluoride membrane, following which the membrane was blocked with 5% non-fat dry milk in 0.1% Tween-20 in PBS (PBST) for 2 h at room temperature. The membrane was subsequently incubated with primary antibodies in PBST overnight at 4˚C, and then incubated with the corresponding secondary antibodies at room temperature for 1 h. The antibodies used in this study included: Anti-PPP2R2D (1:500; cat. no. 181071; Abcam), anti-FLAG (1:2,000; cat. no. F1804; Sigma-Aldrich; Merck KGaA), anti-PPP2CA (1:500; cat. no. 2038), mTOR (1:500; cat. no. 2983), phosphorylated (p)-mTOR (Ser2448) (1:500; cat. no. 9864), protein kinase B (Akt; 1:1,000; cat. no. 9272), p-Akt (1:500; cat. no. 4051), extracellular signal-regulated kinase (Erk; 1:500; cat. no. 4695), p-Erk (1:500; cat. no. 4376) (all from Cell Signaling Technology, Inc., Danvers, MA, USA), β-actin (1:500; cat. no. 81171; Santa Cruz Biotechnology, Dallas, TX, USA) and IRDye 800DX-conjugated, affinity-purified goat anti-rabbit or goat anti-mouse secondary antibodies (#611-145-002 and

#610-145-002, 1:1,000; Rockland Immunochemicals, Inc., Pottstown, PA, USA). The Odyssey Infrared imaging system (LI-COR Biosciences, Lincoln, NE, USA) was then used for detection of the immunoreactive signal.

RNA interference and PPP2R2D overexpression plasmid. In order to silence the expression levels of PPP2R2D or PPP2CA in GC cell lines, small interfering RNA (siRNA) oligonucleotides against PPP2R2D and PPP2CA were chemically synthesized (GenePharma Co., Ltd., Shanghai, China). The siRNAs sequences used were as follows: si-2R2D-1, 5'-GCACCUUUC AAAGUCAUGAdTdT-3'; si-2R2D-2, 5'-GCUCUCUCUAUG AGAACGAdTdT-3'; si-PPP2CA, 5'-CAUGGAACUUGACGA UACUdTdT-3'; and a nonspecific control (si-NC, 5'-UUCUCC GAACGUGUCACGUdTdT-3'. Furthermore, in order to induce overexpression of PPP2R2D, pEnter-PPP2R2D (GenBank accession no. NM_018461) was purchased from Vigene Biosciences, Inc. (Jinan, China). Cells were seeded at 30% confluence (for siRNA transfection) or 80% confluence (for plasmid transfection) into 6-well plates prior to the transfection, and then Lipofectamine® 3000 (Invitrogen; Thermo Fisher Scientific, Inc., Waltham, MA, USA) was used to transfect cells at 37˚C for 48 h with the plasmids or siRNAs according to the manufacturer's protocol. In order to obtain stably transfected cells, a lentivirus knocking down PPP2R2D (LV-sh2R2D) or a lentivirus control (LV-shNC) was generated and purchased from GenePharma Co., Ltd., using the corresponding aforementioned sequences (si-2R2D-1 and si-NC). The cells stably infected with the lentivirus particles were enriched in the culture medium by puromycin screening (Selleck Chemicals, Houston, TX, USA).

Cell proliferation assay. For the cell counting kit-8 (CCK-8) assay, transfected GC cells were seeded into a 96-well culture plate at a density of $3x10^3$ cells per well. At 24, 48, 72, 96 and 120 h after transfection, cells were incubated with 10 μl CCK-8 reagent (Dojindo Molecular Technologies, Inc., Kumamoto, Japan) for 1 h at 37˚C, and then the absorbance of each well was measured spectrophotometrically at 450 nm in an automated plate reader. The results were plotted as the mean ± standard deviation of three independent experiments with five replicates per experiment for each experimental condition.

Colony formation assay. Stably infected GC cells were seeded in a 6-well plate at a density of $1x10^3$ cells per well and cultured for 2-3 weeks, following which the colonies formed were stained with crystal violet for 10 min. Images of the colonies were captured, and the number of cells was counted. All the experiments were performed in triplicate and repeated at least for three times.

5-Ethynyl-2'-deoxyuridine (EdU) incorporation assay. GC cells were seeded at $1.5x10^5$ cells/well in a 6-well plate and cultured for 24 h after transfection with PPP2R2D-expressing plasmids. Subsequently, the cells were incubated with 50 mM EdU for 2 h at room temperature. Following staining with Apollo® 567 (both from RiboBio Co., Ltd., Guangzhou, China) according to the manufacturer's protocol, the cells were observed with an inverted fluorescence microscope and images were captured.

Cell migration assay. Cell migration assays were conducted using a 24-well Transwell chamber (pore size, 8 μm; Costar; Corning, Inc.). Briefly, at 24 h after transfection with plasmids or siRNAs, GC cells were harvested and suspended in DMEM without FBS at a density of $1x10^5$ cells/ml. Next, 400 μl of the cell suspension was loaded in the upper chamber, while 800 μl DMEM containing 10% FBS was added to the bottom chamber. Subsequent to incubation for 24 h at 37˚C, the non-migrating cells in the upper chamber were removed with a cotton swab, and the migrated cells on the bottom surface of the filter were fixed in 4% paraformaldehyde at room temperature for 5 min, stained with crystal violet and counted under a phase contrast microscope in five randomly selected fields at a magnification of x200.

Wound healing assay. GC cells were harvested and re-suspended in DMEM medium supplemented with 10% FBS in a 6-well plate at ~100% confluence. A plastic tip was used to scratch a cell monolayer, and then PBS was used to wash the samples and remove any cell debris, followed by culturing of the cells in serum-free DMEM. After 0, 24 and 48 h, the cells were observed and images were captured using an inverted microscope equipped with a camera.

Animal experiments. In order to establish a xenograft model of GC, 26 nude mice (BALA/c; age, 4-weeks-old) were purchased from Sippr-BK Lab Animal Co., Ltd. (Shanghai, China). Mice were housed for 1 week in a specific-pathogen-free environment prior to injection, under the following standard conditions: 12-h light/dark cycle; temperature, 25˚C; humidity, 40-60%; free access to irradiated food and autoclaved distilled water . A total of $2x10^6$ stably transfected cells in 100 μl PBS, namely MGC803-LV-shNC, MGC803-LV-sh2R2D, MKN28-LV-shNC and MKN28-LV-sh2R2D, were subcutaneously injected into the two flanks of each mouse, respectively (n=8 per group). After 4 weeks, mice were euthanized, and tumors were weighted. The weight of the mice was 18-20 g upon purchase, and 25-28 g upon sacrifice, while the maximum diameter of a single tumor was 14 mm. The tumor volumes were calculated using the following equation: Volume = 0.5 x longitudinal diameter x (latitudinal diameter)^2. The maximum volume of a single tumor was 700 mm^3.

For *in vivo* metastasis experiments, $2.5x10^6$ cells (MGC803-LV-shNC and MGC803-LV-sh2R2D) were injected into the tail veins of the nude mice (n=5 per group). After 10 weeks, mice were euthanized and the visible tumor nodules on the lung surface were calculated. The maximum number of metastatic nodules in a mouse was 4, and the maximum diameter of a metastatic nodule was 3 mm. The lung tissues were immobilized in 4% paraformaldehyde, and paraffin sections (8 μm) were made for hematoxylin and eosin staining. All animal handling and experimental procedures were approved by the Ethics Committee of Shanghai East Hospital, Tongji University School of Medicine.

Statistical analysis. All the quantitative data are expressed as the mean ± standard deviation. The two-tailed χ^2 test was used to determine the significance of the difference among the covariates. Survival durations were calculated using

the Kaplan-Meier method and statistical differences were determined by log-rank test. The *in vitro* data were analyzed using Student's t-test (two-tailed) to determine any statistical significance. A P-value of <0.05 was considered to indicate a statistically significant difference.

Results

PPP2R2D is overexpressed in GC and is associated with the progression and prognosis. To investigate the possible role of PPP2R2D in GC, its protein expression level was first analyzed in a tissue microarray consisting of 90 paired of GC tissues and adjacent normal gastric mucosa specimens by an immunohistochemical approach. As shown in Fig. 1A, GC tissues expressed more PPP2R2D compared with that in the paired normal gastric mucosa tissues, as moderate and strong staining of PPP2R2D was observed in a large number of tumor tissues (P<0.01). In addition, following tissue staining, tumor samples were classified into two groups: Weak staining group, which includes the negative and weakly positive groups, and the strong staining group, which includes the moderately and strongly positive groups. PPP2R2D protein was highly expressed in TNM III and IV cancer tissues [P<0.01 (χ^2 test); Fig. 1B], thus indicating that the level of PPP2R2D may increase gradually with GC progression.

The correlation between PPP2R2D expression and the clinicopathological characteristics of 82 patients with available follow-up data was analyzed and summarized in Table I. The data indicated that PPP2R2D expression was positively correlated with disease stage (P=0.003), T classification (P=0.009) and N classification (P=0.010). Notably, PPP2R2D expression was negatively correlated with the OS rate of patients (P<0.05; Fig. 1C), which was in line with the results demonstrated in the Kaplan-Meier survival curves (Fig. 1D). Furthermore, the qPCR results confirmed the upregulation of PPP2R2D in an additional 28 GC tissues obtained at the Shanghai East Hospital as compared with that in the paired adjacent normal tissue. In total, 17/28 (60.7%) paired GC tissues demonstrated >1.5-fold increase in PPP2R2D expression (P<0.05; Fig. 1E). Taken together, these findings suggested that PPP2R2D is upregulated in GC and strongly associated with GC progression and prognosis.

Table I. Correlation of PPP2R2D expression with clinicopathological features of gastric cancer patients (n=82) from GC tissue microarray.

Feature	No. of cases	Weak Staining (-,+)	Strong staining (++,+++)	P-value
Age (years)				
>60	46	25	21	0.384
≤60	36	23	13	
Gender				
Male	64	38	26	0.771
Female	18	10	8	
Differentiation				
Well-differentiated	16	10	6	0.934
Moderately differentiated	24	14	10	
Poorly differentiated	42	24	18	
T classification[a]				
T1 and T2	16	14	2	0.009
T3 and T4	66	34	32	
N classification[a]				
N0	22	18	4	0.010
N1-3	60	30	30	
M classification[a]				
M0	80	48	32	0.180
M1	2	0	2	
Stage				
I and II	40	30	10	0.003
III and IV	42	18	24	

[a]7th American Joint Committee on Cancer TNM system was used for the classification and staging of gastric cancer.

PPP2R2D promotes GC cell proliferation and colony formation in vitro. PPP2R2D protein expression level was examined in several GC cell lines by western blot analysis in order to determine which cell line was more appropriate for use in overexpression or knockdown experiments. The results revealed that PPP2R2D was highly expressed in MGC803, HGC27, AGS and MKN28 cells, whereas it was expressed at relatively low levels in SGC7901and BGC823cells (Fig. 1E).

PPP2R2D expression was knocked down in MGC803, AGS and MKN28 cells by transient transfection with siRNAs against PPP2R2D, and western blot analysis results indicated that si-2R2D-1 markedly decreased PPP2R2D expression compared with the si-NC group (Fig. 2A). Subsequently, CCK-8 assays were conducted to determine the rate of cell growth. As shown in Fig. 2B, knockdown of PPP2R2D by si-2R2D-2 resulted in significantly reduced GC cell growth compared with that in control cells. In addition, stable cell lines were established by infecting with interference lentivirus (LV-sh2R2D or control LV-shNC) in these cells. Colony formation assays revealed that silencing PPP2R2D inhibited the colony formation capacity of GC cells as indicated in Fig. 2C. Furthermore, PPP2R2D overexpression was achieved by transiently transfecting a FLAG-tagged PPP2R2D-expressing plasmid into SGC7901 and BGC823 cells (Fig. 2D). As expected, the overexpression of PPP2R2D markedly promoted cell growth in the two cell lines (Fig. 2D). Consistent with these findings, the results of EdU incorporation assays demonstrated that the percentage of EdU-positive cells increased subsequent to the overexpression of PPP2R2D in SGC7901 cells (Fig. 2E). The data presented in these experiments suggested that PPP2R2D serves a critical role in promoting cell proliferation and colony formation in GC.

PPP2R2D enhances the migratory ability of GC cells in vitro. Given that PPP2R2D expression was correlated with the lymph node metastasis of GC cells (Table I), the study next determined the impact of PPP2R2D knockdown or overexpres-

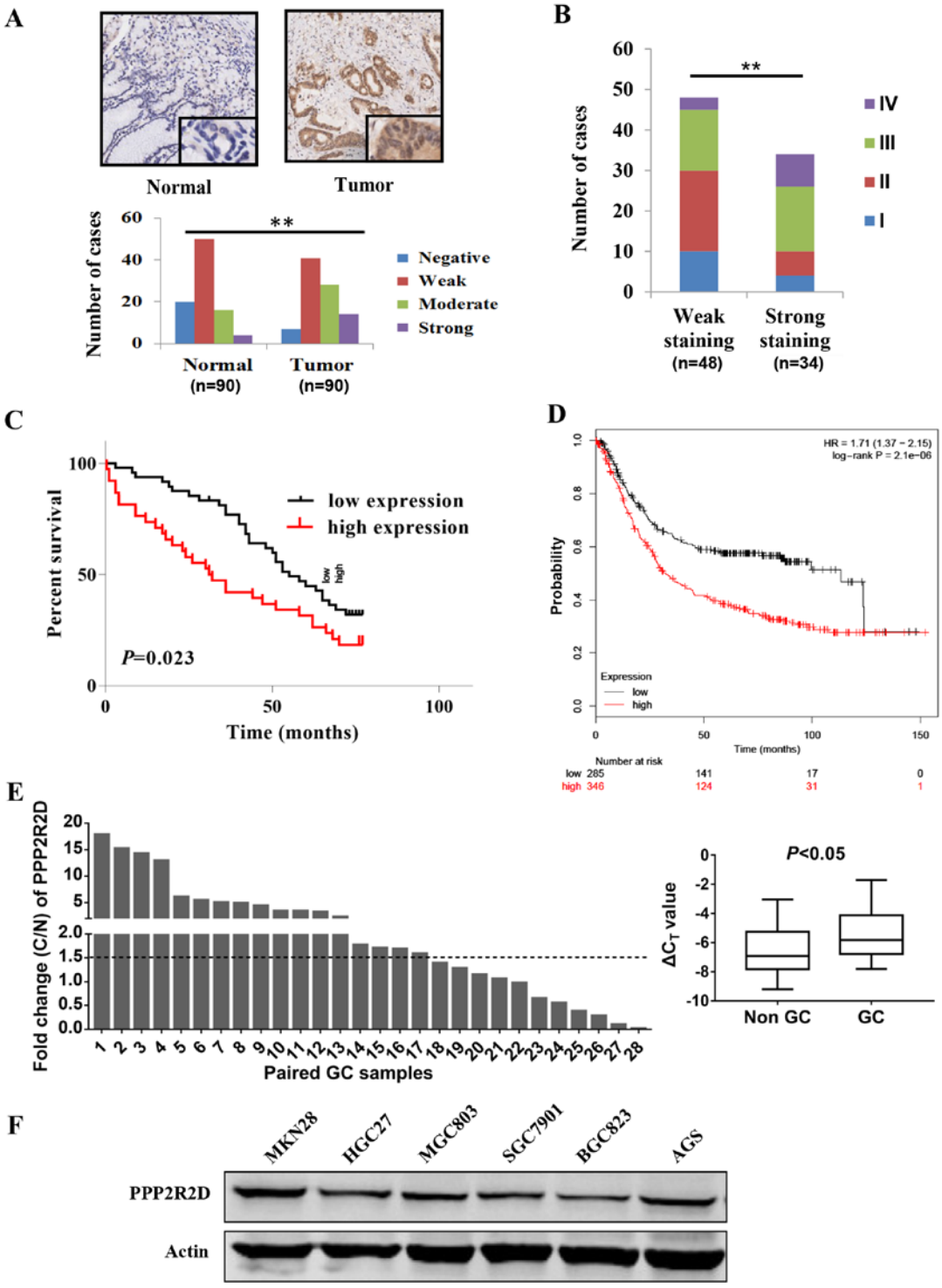

Figure 1. Expression of PPP2R2D in GC specimens and its association with the clinicopathological features of GC. (A) Representative images of PPP2R2D protein expression in a GC specimen and an adjacent normal gastric mucosa specimen (magnification, x40 and x200). (B) Positive association between PPP2R2D expression and disease stage of GC; these data were from the results of a tissue microarray. (C) Kaplan-Meier plot comparing the OS rate in patients with high expression of PPP2R2D (red line; n=38; P<0.05, log-rank test) with those with low expression of PPP2R2D (black line; n=48) based on tissue microarray data. The low expression group includes the negative and weak staining groups, while the high expression group includes the moderate and strong staining groups. (D) OS rate in patients with high expression of PPP2R2D (red line; n=346; P<0.01, log-rank test) was significantly worse in comparison with that in patients with low expression of PPP2R2D (black line; n=285) based on analysis from the Kaplan-Meier Plotter datasets. (E) The mRNA level of PPP2R2D in 28 pairs of GC and non-GC specimens was determined by qPCR. 'C' represents the GC samples and 'N' represents the paired non-GC samples. The box plot (right panel) indicated the difference of PPP2R2D mRNA level in GC samples and non-GC samples (P<0.05). (F) Expression pattern of PPP2R2D protein in different GC cell lines, as determined by western blot analysis. **P<0.01. GC, gastric cancer; OS, overall survival; non-GC, adjacent normal tissue.

sion on GC cell migration via Transwell chamber and wound healing assays. The data from the Transwell assays indicated that silencing PPP2R2D significantly inhibited the migratory ability of GC cells (Fig. 3A), whereas enforced expression of PPP2R2D markedly facilitated the migratory capacity of GC cells (Fig. 3B). Concurrently, PPP2R2D knockdown strongly

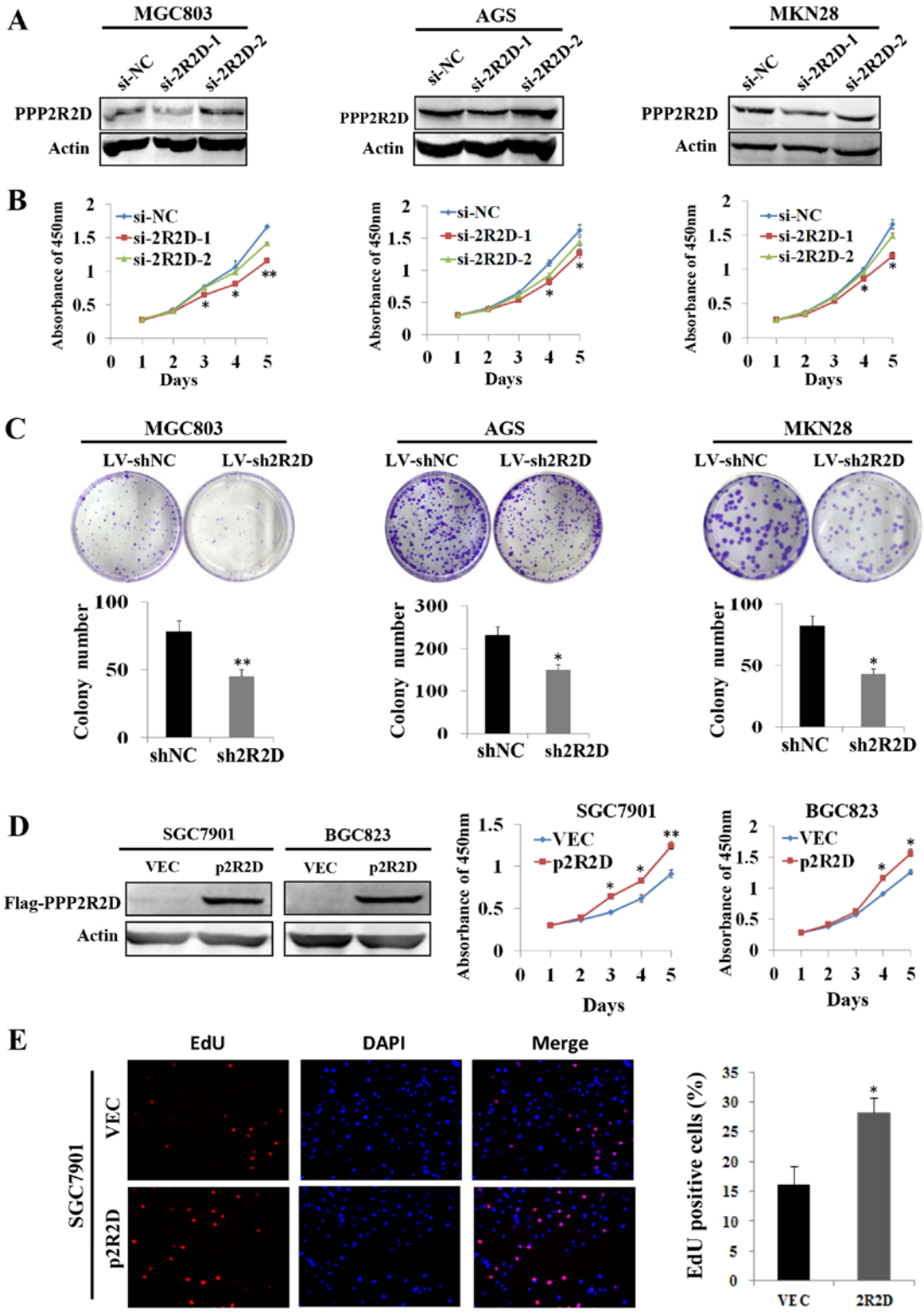

Figure 2. Effect of PPP2R2D expression on GC cell proliferation *in vitro*. (A) The efficiency of PPP2R2D knockdown in MGC803, AGS and MKN28 cells was confirmed by western blot analysis. The effect of PPP2R2D knockdown on (B) cell growth and (C) colony formation ability of GC cells was evaluated by CCK-8 assay and colony formation assay. (D) Cell growth was assessed by CCK-8 method in SGC7901 and BGC823 cells transfected with pEnter-PPP2R2D or VEC. The efficiency of FLAG-tagged pEnter-PPP2R2D expression was determined by western blot analysis with a FLAG antibody. (E) EdU incorporation assay was performed to evaluate the cell proliferation ability of PPP2R2D-overexpressing BGC823 cells. VEC was used as a control vector. Magnification, x100. All data are represented as the mean ± standard deviation of three independent experiments. *P<0.05 and **P<0.01 vs. corresponding control group. GC, gastric cancer; CCK-8, cell counting kit-8; EdU, 5-ethynyl-2'-deoxyuridine; VEC, pEnter empty vector.

restricted the motility of MGC803 and AGS cells towards the wound (Fig. 3C). Therefore, these results indicated that PPP2R2D promotes GC cell migration *in vitro*.

Silencing of PPP2R2D attenuates tumorigenicity and metastasis of GC cells in vivo. The effect of PPP2R2D expression on GC cell tumorigenicity was also evaluated in a nude mouse

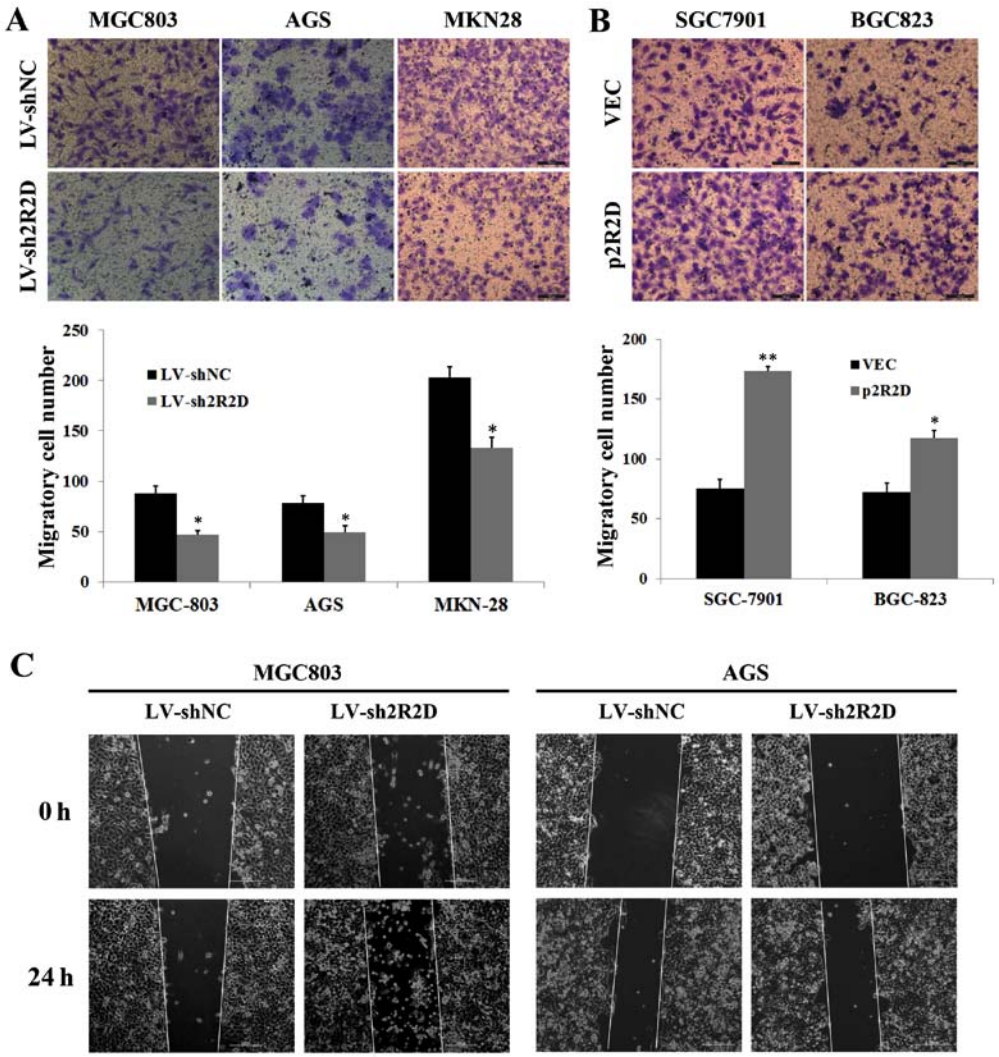

Figure 3. Suppression of gastric cancer cell migration by PPP2R2D knockdown *in vitro*. (A) Representative images and graphs demonstrating the migration ability of MGC803, AGS and MKN28 cells infected with LV-sh2R2D or control LV-shNC. (B) Representative images and graphs demonstrating the migration of PPP2R2D-overexpressing SGC7901 and BGC823 cells. VEC was used as a control. Magnification, x200. (C) Wound healing assay was performed to analyze the motility ability of MGC803 and AGS cells infected with LV-sh2R2D or LV-shNC. Magnification, x100. Data are represented as mean ± SD of three independent experiments. *P<0.05 and **P<0.01 vs. corresponding control group. VEC, pEnter empty vector.

model. The stable knockdown cells (MGC803/LV-sh2R2D and MKN28/LV-sh2R2D) and their corresponding control cells were subcutaneously inoculated into 4-week-old male nude mice (n=8 per group). After 4 weeks, all mice were euthanized and tumors were excised. The results demonstrated that PPP2R2D knockdown significantly suppressed the tumorigenicity of the two GC cells *in vivo*, and the size and weight of tumors were lower compared with those of xenografts formed from control-transfected cells (Fig. 4A). Furthermore, the pulmonary metastasis potential of cells with PPP2R2D knockdown was elucidated by tail vein injection. As expected, no visible metastatic foci were observed on lung surfaces in all 5 mice injected with MGC803/LV-sh2R2D cells. By contrast, 3 out of 5 mice injected with control-transfected cells developed metastatic tumors on the lung surface (Fig. 4B and C). These data further confirmed the oncogenic role of PPP2R2D in animal models.

PPP2R2D influences mTOR phosphorylation level. PP2A holoenzyme is known to serve an essential role in the regulation of critical signaling pathways during tumorigenesis (22,23). Since PPP2R2D is a regulatory subunit of PP2A, the current study attempted to explore whether it is involved in the PP2A-associated signaling pathways. Western blot analysis results revealed that the phosphorylation level of mTOR (p-mTOR) was evidently reduced following knockdown of PPP2R2D in MGC803 and AGS cells, whereas no visible change occurred on the level of p-Akt and p-Erk proteins (Fig. 5A). By contrast, overexpression of PPP2R2D markedly increased the level of p-mTOR without altering the abundance of total mTOR proteins in SGC7901 cells (Fig. 5A). Furthermore, the phosphorylation levels of these three kinases were elevated when PPP2CA, the catalytic subunit of PP2A, was knocked down in GC cells (Fig. 5B), which is in accordance with previous findings (24). Notably, knockdown of PPP2CA did not affect p-mTOR level in the PPP2R2D silenced cells (Fig. 5C), suggesting that the effect of PPP2R2D on p-mTOR level was independent of PPP2CA. Taken together, these results suggested that PPP2R2D contributes to GC progression putatively via mTOR activation.

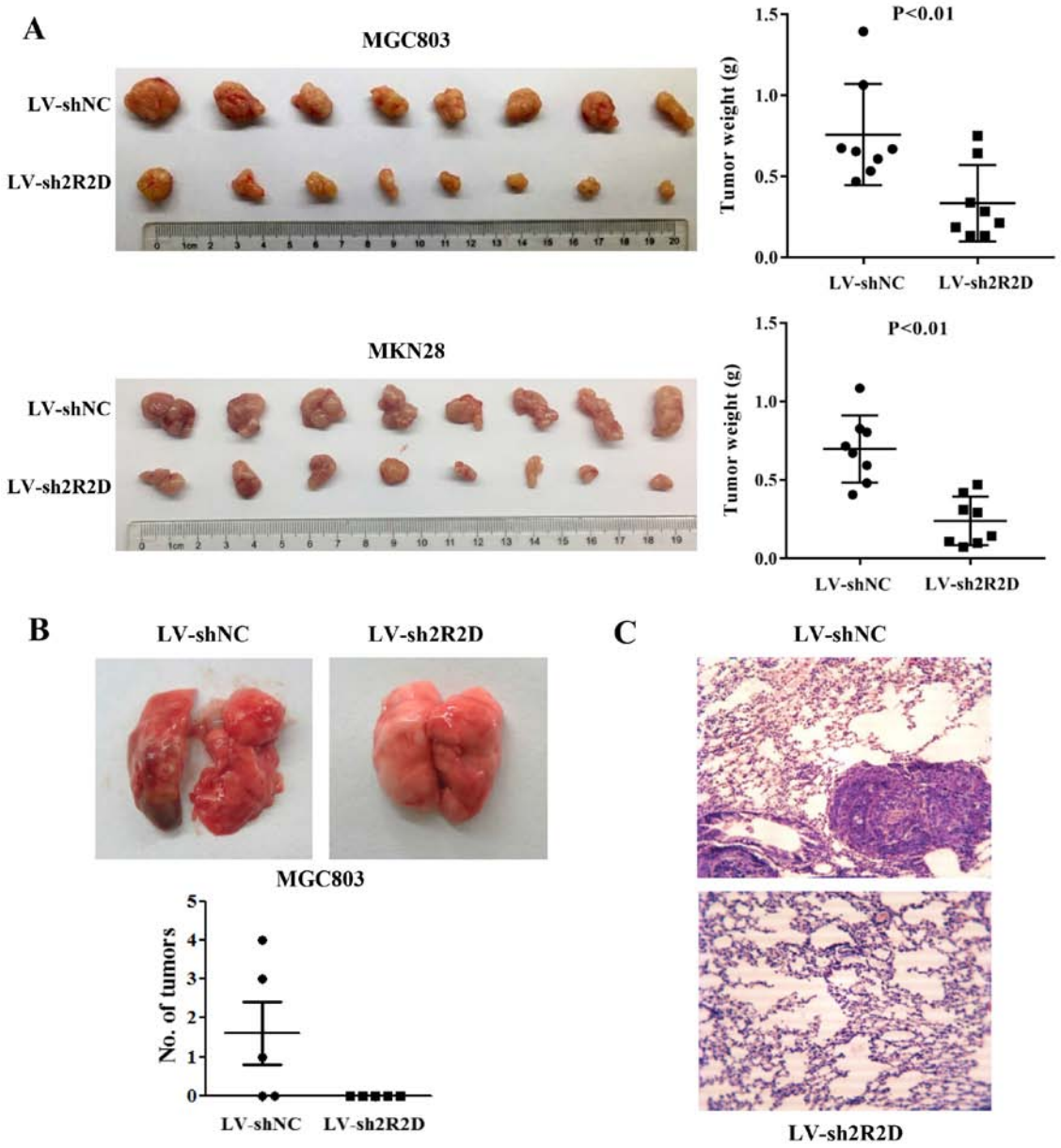

Figure 4. Attenuation of tumorigenicity and metastasis of gastric cancer cells by silencing of PPP2R2D *in vivo*. (A) MGC803 and MKN28 cells infected with LV-sh2R2D or LV-shNC were subcutaneously injected into nude mice (n=8 per group). Tumors were removed and weighted at 4 weeks after injection. (B) Representative images of lung metastases in nude mice and the number of tumor nodules in each group was shown. The lung tissues were removed 10 weeks after injection of $2.5x10^6$ MGC803 cells infected with LV-sh2R2D or LV-shNC into nude mice through the tail veins (n=5 per group). (C) Hematoxylin and eosin-stained sections of lung tissues from the mice are shown (magnification, x200). Data are expressed as the mean ± standard deviation.

Discussion

PPP2R2D, also known as B55δ, is a crucial regulatory subunit of PP2A. Previous studies have reported that PPP2R2D is involved in the regulation of DNA repair (25), while PPP2R2D knockdown inhibited T cell apoptosis and enhanced T cell proliferation, as well as cytokine production in tumors (26). In addition, PPP2R2D has been demonstrated to be associated with specific types of human cancer (16,17). However, the expression and precise function of PPP2R2D in GC have not yet been elucidated.

In the present study, compelling evidence was provided demonstrating an oncogenic role of PPP2R2D in GC progression and development for the first time, to the best of our knowledge. At the cellular level, PPP2R2D promotes GC cell proliferation, colony formation and cell migration. Furthermore, PPP2R2D significantly facilitated the tumorigenicity and metastasis in nude mice. Clinically, PPP2R2D expression was significantly upregulated at the mRNA and protein levels in GC specimens. Immunostaining results also indicated that PPP2R2D expression was positively associated with GC disease stage, T classification and N classification. Notably, a high expression of PPP2R2D was correlated with poor prognosis of patients with GC. Thus, the current study may provide a good indicator for GC progression and prognosis. Furthermore, the clinical data obtained in the present study were in agreement with the findings of the cellular and animal experiments on the physiological function of PPP2R2D.

A number of studies have reported that B subunits direct PP2A towards the regulation of signaling pathways

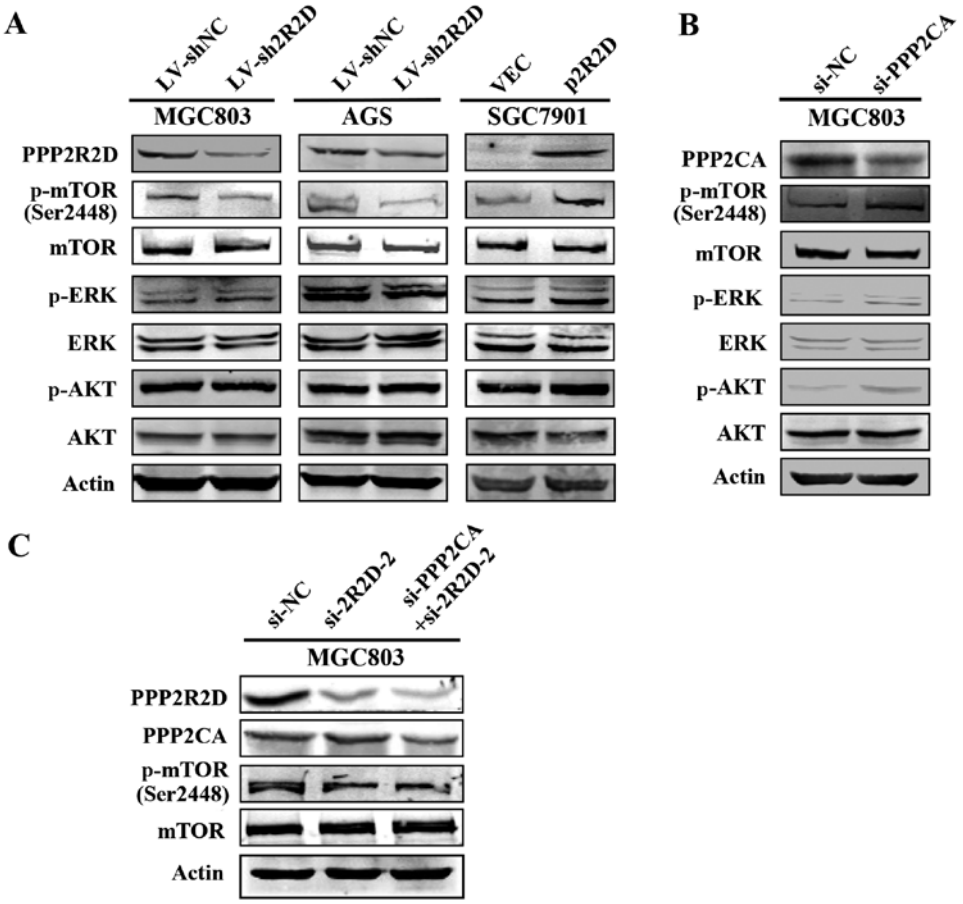

Figure 5. mTOR activation by PPP2R2D overexpression in gastric cancer cells. (A) Western blot results demonstrating the effects of PPP2R2D on the phosphorylation level of mTOR, Akt and Erk proteins. MGC803 and AGS cells were infected with LV-sh2R2D or control LV-shNC, while SGC7901 cells were transfected with FLAG-tagged plasmids or VEC. (B) Silencing PPP2CA significantly enhanced the phosphorylation of mTOR, Akt and Erk proteins in MGC803 cells. (C) Knockdown of PPP2R2D and PPP2CA in MGC803 cells via si-2R2D and si-PPP2CA, respectively. Western blot analysis was performed to investigate whether PPP2CA knockdown had an effect on PPP2R2D-mediated mTOR phosphorylation. mTOR, mechanistic target of rapamycin; Akt, protein kinase B; extracellular signal-regulated kinase; p-, phosphorylated; VEC, pEnter empty vector.

that control the cell cycle progression, cell proliferation and apoptosis in eukaryotes (27-29). mTOR is one of the critical kinases involved in the regulation of numerous cellular events, including cell proliferation, protein synthesis, migration, angiogenesis and metastasis in normal and cancer cells (30-33). In addition, the PI3K/Akt/mTOR signaling pathway is known to be regulated by phosphatases such as PP2A (24,34). Nevertheless, a direct link between PPP2R2D and mTOR in tumor development has yet to be established. In the current study, the PPP2R2D-mediated phosphorylation of mTOR protein at serine 2448 was described, which may be independent of the PP2A catalytic subunit PPP2CA as determined by western blot analysis. The current results also indicated that PPP2R2D is endowed with tumor-promoting capacity via an increased level of active mTOR. Notably, unlike PPP2CA, overexpression and knockdown of PPP2R2D did not exert any significant effects on Akt and Erk phosphorylation, implying that the involvement of PPP2R2D in mTOR activation varies in the case of Akt or Erk activation. However, how PPP2R2D regulates the mTOR phosphorylation remains unclear, and its association with PPP2CA would also be worth exploring in future studies.

In conclusion, the results of the cell biological experiments and analysis of clinical data in the present study consistently indicated that the expression of PPP2R2D serves pivotal roles in GC progression and metastasis. In addition, mTOR signaling may mediate the oncogenic roles of PPP2R2D. The current observations also provided a new insight into the link between regulatory subunits of PP2A and tumor development. Taken together, PPP2R2D may serve as a new independent prognostic indicator and therapeutic target for GC treatment.

Acknowledgements

Not applicable.

Funding

This study was supported by grants from the National Natural Science Foundation of China (nos. 81772567, 81272917 and 81302064), and the Outstanding Leaders Training Program of Pudong Health Bureau of Shanghai (no. PWRl2013-02).

Availability of data and materials

The data and materials used and/or analyzed during the current study are available from the corresponding author on reasonable request.

Authors' contributions

YL and YG conceived and designed the study. SY, LL and QW acquired, analyzed and interpreted the data. SY and YL wrote and reviewed the manuscript. ND cultured all of the cell lines, and performed cell transfection and lentiviral infection experiments. All authors read and approved the final manuscript.

Ethics approval and consent to participate

The experiments were approved by the Ethics Committee of Shanghai East Hospital, Tongji University School of Medicine (Shanghai, China). Informed consent was obtained from all patients prior to the sample collection.

Consent for publication

The patient, or parent, guardian or next of kin provided written informed consent for the publication of any associated data and accompanying images.

Competing interests

The authors declare that they have no competing interests.

References

1. Hunter T: Protein kinases and phosphatases: The yin and yang of protein phosphorylation and signaling. Cell 80: 225-236, 1995.
2. Janssens V and Goris J: Protein phosphatase 2A: A highly regulated family of serine/threonine phosphatases implicated in cell growth and signalling. Biochem J 353: 417-439, 2001.
3. Lechward K, Awotunde OS, Swiatek W and Muszyńska G: Protein phosphatase 2A: Variety of forms and diversity of functions. Acta Biochim Pol 48: 921-933, 2001.
4. Virshup DM: Protein phosphatase 2A: A panoply of enzymes. Curr Opin Cell Biol 12: 180-185, 2000.
5. Sontag E: Protein phosphatase 2A: The Trojan Horse of cellular signaling. Cell Signal 13: 7-16, 2001.
6. Seshacharyulu P, Pandey P, Datta K and Batra SK: Phosphatase: PP2A structural importance, regulation and its aberrant expression in cancer. Cancer Lett 335: 9-18, 2013.
7. Strack S, Chang D, Zaucha JA, Colbran RJ and Wadzinski BE: Cloning and characterization of B delta, a novel regulatory subunit of protein phosphatase 2A. FEBS Lett 460: 462-466, 1999.
8. Mayer RE, Hendrix P, Cron P, Matthies R, Stone SR, Goris J, Merlevede W, Hofsteenge J and Hemmings BA: Structure of the 55-kDa regulatory subunit of protein phosphatase 2A: Evidence for a neuronal-specific isoform. Biochemistry 30: 3589-3597, 1991.
9. Zolnierowicz S, Csortos C, Bondor J, Verin A, Mumby MC and DePaoli-Roach AA: Diversity in the regulatory B-subunits of protein phosphatase 2A: Identification of a novel isoform highly expressed in brain. Biochemistry 33: 11858-11867, 1994.
10. Janssens V, Goris J and Van Hoof C: PP2A: The expected tumor suppressor. Curr Opin Genet Dev 15: 34-41, 2005.
11. Li W, Xie L, Chen Z, Zhu Y, Sun Y, Miao Y, Xu Z and Han X: Cantharidin, a potent and selective PP2A inhibitor, induces an oxidative stress-independent growth inhibition of pancreatic cancer cells through G2/M cell-cycle arrest and apoptosis. Cancer Sci 101: 1226-1233, 2010.
12. Schweyer S, Bachem A, Bremmer F, Steinfelder HJ, Soruri A, Wagner W, Pottek T, Thelen P, Hopker WW, Radzun HJ, *et al*: Expression and function of protein phosphatase PP2A in malignant testicular germ cell tumours. J Pathol 213: 72-81, 2007.
13. Duong FH, Dill MT, Matter MS, Makowska Z, Calabrese D, Dietsche T, Ketterer S, Terracciano L and Heim MH: Protein phosphatase 2A promotes hepatocellular carcinogenesis in the diethylnitrosamine mouse model through inhibition of p53. Carcinogenesis 35: 114-122, 2014.
14. Lu J, Kovach JS, Johnson F, Chiang J, Hodes R, Lonser R and Zhuang Z: Inhibition of serine/threonine phosphatase PP2A enhances cancer chemotherapy by blocking DNA damage induced defense mechanisms. Proc Natl Acad Sci USA 106: 11697-11702, 2009.
15. Boudreau RT, Conrad DM and Hoskin DW: Apoptosis induced by protein phosphatase 2A (PP2A) inhibition in T leukemia cells is negatively regulated by PP2A-associated p38 mitogen-activated protein kinase. Cell Signal 19: 139-151, 2007.
16. Zhuang Q, Zhou T, He C, Zhang S, Qiu Y, Luo B, Zhao R, Liu H, Lin Y and Lin Z: Protein phosphatase 2A-B55δ enhances chemotherapy sensitivity of human hepatocellular carcinoma under the regulation of microRNA-133b. J Exp Clin Cancer Res 35: 67, 2016.
17. Cunningham CE, Li S, Vizeacoumar FS, Bhanumathy KK, Lee JS, Parameswaran S, Furber L, Abuhussein O, Paul JM, McDonald M, *et al*: Therapeutic relevance of the protein phosphatase 2A in cancer. Oncotarget 7: 61544-61561, 2016.
18. Ferlay J, Soerjomataram I, Dikshit R, Eser S, Mathers C, Rebelo M, Parkin DM, Forman D and Bray F: Cancer incidence and mortality worldwide: Sources, methods and major patterns in GLOBOCAN 2012. Int J Cancer 136: E359-E386, 2015.
19. Edge SB; American Joint Committee on Cancer: AJCC Cancer Staging Manual. Springer, New York, 2010.
20. Capes-Davis A, Theodosopoulos G, Atkin I, Drexler HG, Kohara A, MacLeod RA, Masters JR, Nakamura Y, Reid YA, Reddel RR, *et al*: Check your cultures! A list of cross-contaminated or misidentified cell lines. Int J Cancer 127: 1-8, 2010.
21. Livak KJ and Schmittgen TD: Analysis of relative gene expression data using real-time quantitative PCR and the 2(-Delta Delta C(T)) method. Methods 25: 402-408, 2001.
22. Rodgers JT, Vogel RO and Puigserver P: Clk2 and B56β mediate insulin-regulated assembly of the PP2A phosphatase holoenzyme complex on Akt. Mol Cell 41: 471-479, 2011.
23. Zeng Q, Zhang H, Qin J, Xu Z, Gui L, Liu B, Liu C, Xu C, Liu W, Zhang S, *et al*: Rapamycin inhibits BAFF-stimulated cell proliferation and survival by suppressing mTOR-mediated PP2A-Erk1/2 signaling pathway in normal and neoplastic B-lymphoid cells. Cell Mol Life Sci 72: 4867-4884, 2015.
24. Sablina AA, Hector M, Colpaert N and Hahn WC: Identification of PP2A complexes and pathways involved in cell transformation. Cancer Res 70: 10474-10484, 2010.
25. Kalev P, Simicek M, Vazquez I, Munck S, Chen L, Soin T, Danda N, Chen W and Sablina A: Loss of PPP2R2A inhibits homologous recombination DNA repair and predicts tumor sensitivity to PARP inhibition. Cancer Res 72: 6414-6424, 2012.
26. Zhou P, Shaffer DR, Alvarez Arias DA, Nakazaki Y, Pos W, Torres AJ, Cremasco V, Dougan SK, Cowley GS, Elpek K, *et al*: In vivo discovery of immunotherapy targets in the tumour microenvironment. Nature 506: 52-57, 2014.
27. Eichhorn PJ, Creyghton MP and Bernards R: Protein phosphatase 2A regulatory subunits and cancer. Biochim Biophys Acta 1795: 1-15, 2009.
28. Letourneux C, Rocher G and Porteu F: B56-containing PP2A dephosphorylate ERK and their activity is controlled by the early gene IEX-1 and ERK. EMBO J 25: 727-738, 2006.
29. Kuo YC, Huang KY, Yang CH, Yang YS, Lee WY and Chiang CW: Regulation of phosphorylation of Thr-308 of Akt, cell proliferation, and survival by the B55alpha regulatory subunit targeting of the protein phosphatase 2A holoenzyme to Akt. J Biol Chem 283: 1882-1892, 2008.
30. Wullschleger S, Loewith R and Hall MN: TOR signaling in growth and metabolism. Cell 124: 471-484, 2006.
31. Guertin DA and Sabatini DM: Defining the role of mTOR in cancer. Cancer Cell 12: 9-22, 2007.
32. Chen L, Xu B, Liu L, Liu C, Luo Y, Chen X, Barzegar M, Chung J and Huang S: Both mTORC1 and mTORC2 are involved in the regulation of cell adhesion. Oncotarget 6: 7136-7150, 2015.
33. Bai H, Li H, Li W, Gui T, Yang J, Cao D and Shen K: The PI3K/AKT/mTOR pathway is a potential predictor of distinct invasive and migratory capacities in human ovarian cancer cell lines. Oncotarget 6: 25520-25532, 2015.
34. Zhang Q and Claret FX: Phosphatases: The new brakes for cancer development? Enzyme Res 2012: 659649, 2012.